Research Article Vol. 56, No. 15 / May 20 2017 / Applied Optics 4419

applied optics

Utilization of complex-valued signals in a white-light scanning interferometer for accurate measurement of a surface profile

Songjie Luo,[1] Osami Sasaki,[1,2,*] Ziyang Chen,[1] and Jixiong Pu[1]

[1]Fujian Provincial Key Laboratory of Light Propagation and Transformation, College of Information Science and Engineering, Huaqiao University, Xiamen, Fujian 361021, China
[2]Niigata University, Emeritus, Niigat-shi, Niigata 950-2181, Japan
*Corresponding author: osamija@gmail.com

Received 21 February 2017; revised 25 April 2017; accepted 26 April 2017; posted 26 April 2017 (Doc. ID 287093); published 17 May 2017

Complex-valued interference signals (CVISs) of a white-light scanning interferometer (WLSI) and a spectrally resolved interferometer (SRI) are obtained from their real-valued interference signals through Fourier transform. First the phase distribution in the CVIS of the SRI indicates a dispersion phase caused by two sides of unequal length in a cubic beam splitter, and the magnitude of the dispersion phase changes linearly along a horizontal direction of the beam splitter. Next the dispersion phase with a different magnitude is subtracted from the spectral phase in Fourier transform of the CVIS of the WLSI. Through inverse Fourier transform of this spectral distribution, a dispersion-free CVIS is obtained, and the position of zero phase nearest to the position of amplitude maximum provides a surface profile measured accurately with an error less than 4 nm after 2π corrections, while a position calculated by the linear component of the spectral phase causes measurement error less than 12 nm.

OCIS codes: (120.3180) Interferometry; (120.4825) Optical time domain reflectometry; (120.5050) Phase measurement.

https://doi.org/10.1364/AO.56.004419

1. INTRODUCTION

Three-dimensional shape measurements of reflecting surfaces have been made widely by white-light scanning interferometry, and there are different techniques to determine a position of a reflecting surface from the interference signal. A real-valued interference signal is detected, and it has two special values along the scanning position. One is the maximum value of the envelope, which is called envelope peak [1], coherence peak [2], or top of envelope [3]. The other is the maximum value of the interference signal, which is called fringe peak [1] or signal maximum [3]. When there is a dispersion effect and noise effect in the interference between the object and reference beams, the envelope peak and the fringe peak do not exist on the same scanning position. It has been reported that the fringe peak provided better accuracy in position measurement compared with the envelope peak [1,3]. The position of the fringe peak is not completely the same as the position where the phase of the interference signal is zero, because the real-valued interference signal is a product of the envelope function and the cosine function of the phase distribution. Therefore the position of zero phase nearest to the envelope peak is an important position that will provide the exact position of a reflecting surface. From this point of view, the phase distribution around the envelope peak has been calculated by using the phase-shifting method to get accurate surface profiles [2]. Also, comparisons between surface profiles obtained from the coherence peak position and the zero phase position have been presented [4]. The methods described above focus on the waveform of the real-valued interference signal itself, but it is very important to utilize a spectral distribution in wavenumber domain, which is Fourier transform of the real-valued interference signal [5]. The phase in the spectral distribution is a linear distribution when there is no dispersion effect and no noise effect in the interference signal. The slope of the linear component of the phase distribution in wavenumber domain provides a position of the reflecting surface [5–7]. On the other hand, the complex-valued interference signal is obtained through inverse Fourier transform of the spectral distribution. The amplitude and phase distributions of the complex-valued interference signal correspond to envelope and phase distributions of the real-valued interference signal, respectively. In Ref. [8] it is expected that the position of zero phase nearest to the position of maximum amplitude provides an exact position of a reflecting surface after eliminating the dispersion phase in the spectral distribution. The dispersion phase caused by a cubic beam splitter in a white-light scanning interferometer is detected with a spectrally

resolved interferometer. Although the complex-valued interference signal can be calculated by Hilbert transform [2,3,9], Fourier transform is used to get the spectral distribution in wavenumber domain.

In this paper, based on the method of the signal processing in one point detection reported in Ref. [8], an accurate measurement of surface profile is achieved. First, it is made clear with a spectrally resolved interferometer that the magnitude of the dispersion phase caused by a cubic beam splitter has a linear distribution along its horizontal side. And it is shown how to eliminate the dispersion phase from the interference signals of a white-light scanning interferometer detected on a plane of a camera. Next, a surface profile of an optical mirror is measured with a white-light scanning interferometer. In wavenumber domain, the dispersion phase is eliminated and a slope of the linear phase component is calculated. A complex-valued interference signal is obtained through inverse Fourier transform of the dispersion-free spectral distribution, and the position of zero phase nearest to the position of amplitude maximum is obtained. It is verified that the surface profile obtained from the position of zero phase is more accurate than that from the slope of the linear phase component.

2. PRINCIPLE

A. Complex-Valued Interference Signal

Figure 1 shows a Michelson interferometer that has a supercontinuum light source and a piezoelectric transducer (PZT). Position z of the reference surface is moved by the PZT. Denoting the position of object surface by z_o, the optical path difference (OPD) is $L = 2(z - z_o)$. When the PZT moves and an interference signal is detected with a camera, the interferometer is a white-light scanning interferometer (WLSI). The interference signal expressed as a function of the scanning position z is given by

$$S(z) = \int_{-\infty}^{\infty} I(\sigma)\cos[4\pi(z - z_o)\sigma + \varphi(\sigma)]\mathrm{d}\sigma, \quad (1)$$

where σ is the wavenumber, and $I(\sigma)$ is the spectral intensity of the light source. Phase $\varphi(\sigma)$ is an aberration phase. $I(\sigma)$ and $\varphi(\sigma)$ are defined in the region of $\sigma > 0$. By considering only the term of $e^{j4\pi(z-z_0)\sigma + j\varphi(\sigma)}$ generated from the cosine function in Eq. (1), the Fourier transform of $S(z)$ in the region of positive wavenumbers is derived as

$$F(\sigma) = I(\sigma)e^{j\varphi(\sigma)}e^{-j4\pi z_o\sigma}(\sigma > 0). \quad (2)$$

Expressing the inverse Fourier transform of $I(\sigma)e^{j\varphi(\sigma)}$ by $A(L)e^{j\alpha(L)}$, the complex-valued interference signal (CVIS) is given by

$$S_c(z) = A(2z - 2z_o)\exp[j\alpha(2z - 2z_o)]. \quad (3)$$

Equations (2) and (3) lead to the following characteristic: when $\varphi(\sigma)$ is not equal to zero, a position z_a of maximum amplitude of $A(L)$ and a position z_p of zero phase of $\alpha(L)$ are not identical, and they are not equal to a position z_o of an object surface. In Eq. (2) a slope g of the linear component of the phase distribution is calculated to obtain a measurement value $z_s = -g/4\pi$. Since the aberration phase $\varphi(\sigma)$ contains a dispersion phase, the dispersion phase is detected with a spectrally resolved interferometer (SRI) to reduce the aberration phase close to zero value.

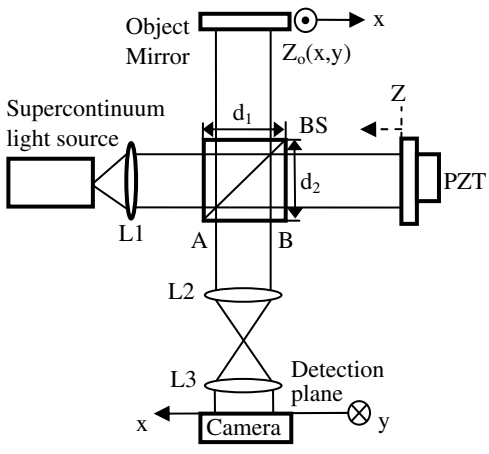

Fig. 1. Schematic of a white-light scanning interferometer.

B. Detection of Dispersion Phase with Spectrally Resolved Interferometer

When the camera is replaced with a face of an optical fiber connecting to a spectral analyzer and the PZT is stationary in Fig. 1, the interferometer is a SRI. The interference signal expressed as a function of $L = 2z - 2z_o$ is given by

$$S_s(\sigma) = I(\sigma)\cos[2\pi L\sigma + \varphi_d(\sigma)], \quad (4)$$

where $\varphi_d(\sigma)$ is a dispersion phase. This dispersion phase is caused by a cubic beam splitter that has two sides whose lengths are d_1 and d_2, respectively, and $d_e = d_1 - d_2$ as shown in Fig. 1. The two beams generating the interference signal pass through a point on the exit side of the beam splitter denoted by the line A-B along the x axis. Defining a coefficient γ whose value changes linearly from 0 to 1 along the line A-B or the coordinate of x, then the dispersion phase is given by

$$\varphi_d(\sigma) = 4\pi[n(\sigma) - 1]\gamma d_e\sigma, \quad (5)$$

where $n(\sigma)$ is the refractive index. The dispersion phase does not depend on the coordinate of y. The amplitude $I(\sigma)$ and the phase $\varphi_d(\sigma)$ can be obtained by deriving the complex-valued signal of $S_s(\sigma)$ through Fourier transform of Eq. (4) in the same way as the CVIS of Eq. (3) is derived.

C. Elimination of Dispersion Phase in Surface Profile Measurement

A measured dispersion phase is denoted by $\varphi_{d,b}(\sigma)$ after linear and bias components are eliminated from a dispersion phase $\varphi_d(\sigma)$ detected at one position around the center of the detection plane. Linear and bias components are eliminated from the aberration phase $\varphi(\sigma)$ obtained from the interference signal of the WLSI detected at one point of (x, y) on the detection plane. This aberration phase without linear and bias components is denoted by $\varphi_x(\sigma)$. It is assumed that the sum of the absolute differences of $|\varphi_x(\sigma) - w_x\varphi_{d,b}(\sigma)|$ over the wavenumber σ has a minimum value when the value of w_x is equal to $W(x)$ as a function of x. In experiments $W(x)$ is not completely a linear function of x, and a value of $W(x)$ increases nearly in proportional to x as the coordinate of x decreases. If the linear component of $W(x)$ is expressed by $ex + e_0$, the dispersion phase,

which should be subtracted from $\varphi(\sigma)$ detected at a point of x, is given by

$$\varphi_{d,x}(\sigma) = (ex + e_0)\varphi_{d,b}(\sigma). \quad (6)$$

3. EXPERIMENT

A. Detection of Dispersion Phase

Figure 1 shows the experimental setup. Both the object and reference surfaces were uncoated optical mirrors with flatness of one-eighth wavelength. The mirrors were regarded as one reflecting surface. The two optical fields existing on the object and reference surfaces, respectively, were made with the two lenses of L2 and L3 with unity magnification on the detection plane. The light source of the interferometer was a supercontinuum light source whose spectral range of a supercontinuum light source was 500 nm–1400 nm. This large spectral width causes a dispersion phase in the interference signal because of the different length d_e between the two sides of the cubic beam splitter (BS), as described in Section 2.B. The camera was replaced with a spectral analyzer to detect the dispersion phase on the detection plane with a SRI. The position of the face of an optical fiber connecting to the spectral analyzer was changed as shown in Fig. 2. The interval of the detection points was 4 mm. The x axis corresponds to the line A-B whose length was 25 mm. Detection point b was about on the center of the x–y surface of the BS.

First the interference signal of the SRI was detected at point b as shown in Fig. 3. The wavenumber range of the interference signal was 1.1–2.1 μm^{-1} and the data number of the interference signal was 1024. Fourier transform was performed on the interference signal. A rectangular window was multiplied by the Fourier transform of the interference signal to choose the positive part. And inverse Fourier transform was performed on this windowed data to get the CVIS. Since the amplitude distribution of the CVIS was almost zero outside the wavenumber region of 1.15–2.0 μm^{-1}, a linear component and a bias component were eliminated from the phase distribution of the CVIS in the region of 1.15–2.0 μm^{-1} to get the dispersion phase shown in Fig. 4(b). Next, when the detection point was moved to the two points along the y axis, the detected dispersion phases were almost the same as that detected at point b. Figure 4(c) shows the dispersion phase detected at point c. Finally, when the detection point was moved to the five points along the x axis, the magnitude of the detected dispersion phases was nearly proportional to the coordinate value of the x axis while its waveform almost did not change. Figure 4(a) shows the dispersion phase detected at point a.

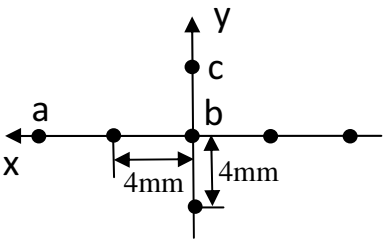

Fig. 2. Measurement points in the SRI on the detection plane.

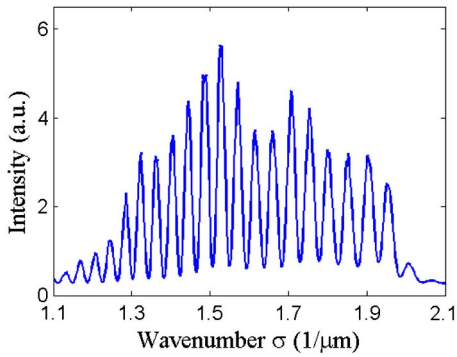

Fig. 3. Interference signal of the SRI detected at point b.

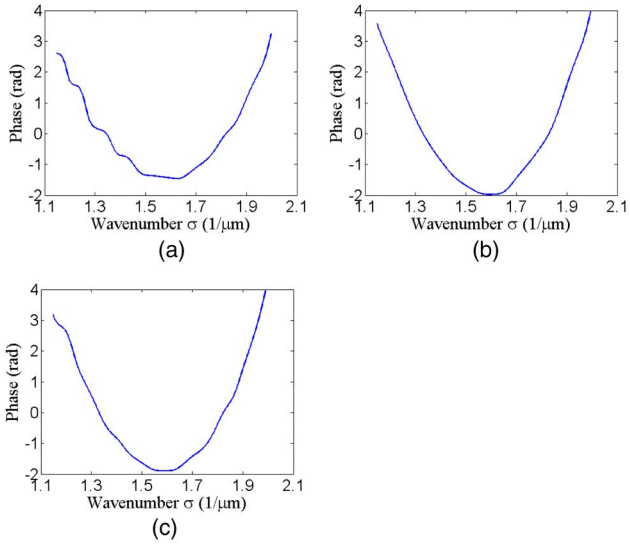

Fig. 4. Dispersion phase distributions detected at different detection points; (a) point a, (b) point b, and (c) point c.

It has been made clear that the magnitude of the dispersion phase changes along the x axis and does not change along the y axis. In order to eliminate the dispersion phase in surface profile measurements, a distribution of the dispersion phase along the x axis was made by using the dispersion phase detected at point b as $\varphi_{d,b}(\sigma)$, which was defined in Section 2.C. The measurement point on the camera along the x axis was expressed by $x = N_x\Delta x$ in Eq. (6), where N_x was the number of the measurement points and Δx was its interval. Since the values of e and e_0 were $-0.0083/\Delta x$ and 1.25, respectively, Eq. (6) was rewritten as

$$\varphi_{d,x}(\sigma) = (1.25 - 0.0083N_x)\varphi_{d,b}(\sigma). \quad (7)$$

B. Surface Profile Measurement

A high-speed camera was used as the detector and its pixel size was 20 μm × 20 μm. The frame size was 640 × 480 pixels. An interference signal detected on one pixel was used in the region of 10 × 10 pixels, and the measurement points of 56 × 41 pixels with the interval of 200 μm were made for the surface profile measurement. The measuring points were denoted by N_x and

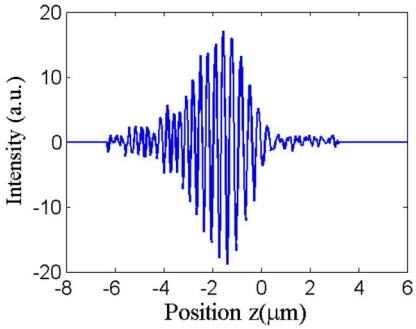

Fig. 5. Interference signal detected at a measurement point of $N_x = 30$ and $N_y = 18$ on the camera.

N_y. N_x was from 1 to 56, and N_y was from 1 to 56. The reference surface was moved by the PZT at a constant velocity of about 80 μm/s, and the sampling interval Δz of the interference signal was 39.6 nm in the scanning white-light interferometer. The data number N of the detected interference signal was 1024, and a required interference signal was selected with a rectangular window whose data number was 240. The other data outside the window were zero values. Figure 5 shows the windowed interference signal detected at a measurement point of $N_x = 30$ and $N_y = 18$, nearly equal to point b in Fig. 2. Fourier transform was performed on this windowed interference signal of data number $N = 1024$. The variable in the Fourier transform of the interference signal was wavenumber σ and its interval was $\Delta\sigma = 1/(2N\Delta z) = 0.0123\ \mu m^{-1}$. Figures 6(a) and 6(b) show amplitude and phase of the Fourier transform of the interference signal, respectively. Amplitude

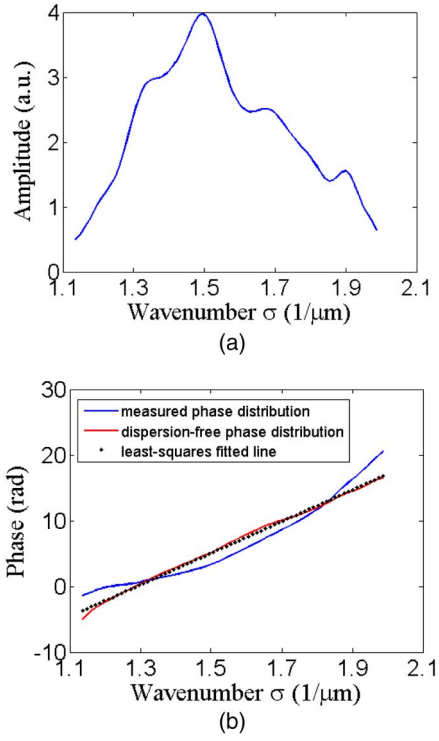

Fig. 6. Fourier transform of the interference signal of Fig. 5; (a) amplitude and (b) phase.

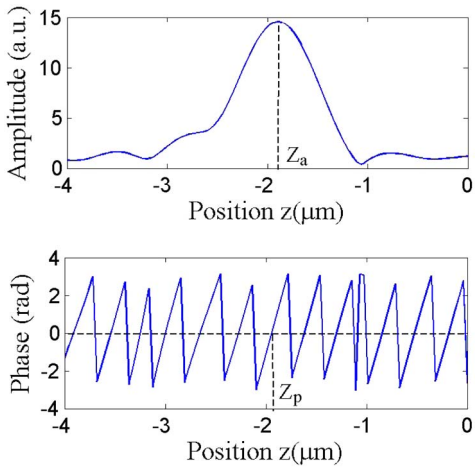

Fig. 7. Complex-valued interference signal of Fig. 5 at $N_x = 30$ and $N_y = 18$ after eliminating the dispersion phase. $z_a = -1.898$ μm and $z_p = -1.940$ μm.

was almost zero outside the wavenumber range of 1.15–2.0 μm^{-1}. The blue line in Fig. 6(b) was the measured phase distribution. The dispersion phase given by Eq. (7) was subtracted from the blue line to get the dispersion-free phase shown by the red line. Since the dispersion-free phase is nearly equal to a linear line, a least square fitted line was calculated as shown by the dotted line. A measurement value z_s of the object position was obtained as $z_s = -g/4\pi$ as described in Section 2.A. By performing inverse Fourier transform on the complex-valued data of the amplitude and the dispersion-free phase of Fig. 6, the CVIS was obtained as shown in Fig. 7. The position of maximum amplitude was denoted by z_a, and the position z_p of zero phase nearest to z_a was another measurement value obtained from the phase distribution in the CVIS. In Fig. 7 the position z_a of −1.898 μm determined the measured position z_p of −1.940 μm.

The signal processing to obtain the two measurement values of z_s and z_p was carried out for all of the measurement points to get surface profiles of the optical mirror. The dispersion phase to be subtracted from the spectral phase detected at a measurement point of N_x was given by Eq. (7). A surface profile obtained from the measured values of z_s is shown in Fig. 8, where the tilt and piston components were eliminated. Small variations with the magnitude less than 12 nm exist, and spike-like large variations appear in the upper-left corner due to small amplitudes of the interference signals. In order to confirm clearly these small variations, Fig. 9 shows one-dimensional distribution along N_x at $N_y = 20$ in the surface profile of Fig. 8. A surface profile obtained from measured values of z_p is shown in Fig. 10, where the tilt and piston components were eliminated. There are many step-like variations whose width was about 0.320 μm. The value of 0.640 μm was nearly equal to the weighted average wavelength 0.638 μm in Fig. 6(a). The three regions indicated with A, B, and C in Fig. 10 are distinguished by the two boundaries where the step change in z_o value occurred. In Fig. 7 one period in the wrapped phase distribution was also about 0.320 μm around the position of z_a. The CVIS obtained at a measurement point of $N_x = 40$ and $N_y = 18$ is

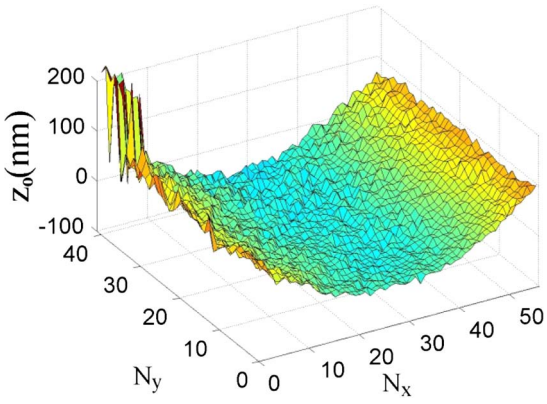

Fig. 8. Surface profile obtained from the measured values of z_s.

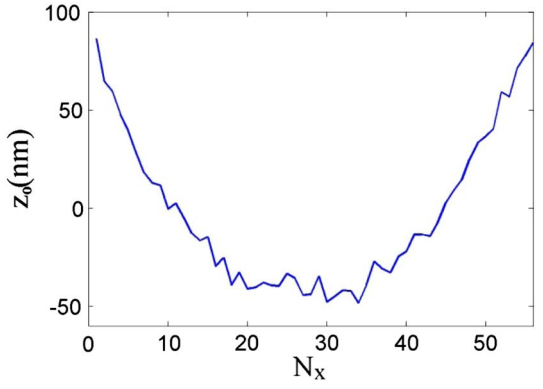

Fig. 9. One-dimensional distribution along N_x at $N_y = 20$ in the surface profile of Fig. 8.

shown in Fig. 11 to be compared with Fig. 7 and to examine how the step change occurred in Fig. 10. In Fig. 11 the position z_a of −1.819 μm determined the measured position z_p of −1.663 μm, where the difference between the two positions was 0.156 μm. Hence the step change in the measured position z_p was caused by the situation that in the region B the position of z_a always existed on the right-hand of an exact position of z_p at a distance more than 0.160 μm. Similarly, in the region C the

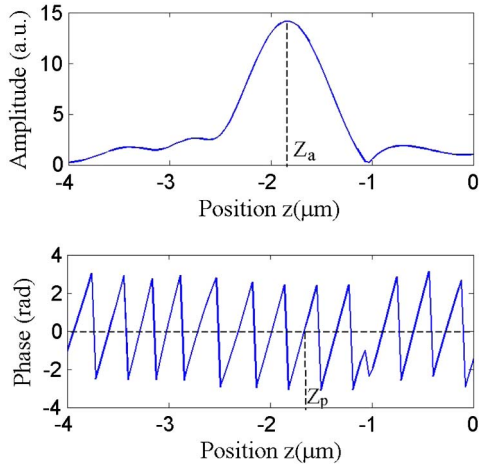

Fig. 11. Complex-valued interference signal at a measurement point of $N_x = 40$ and $N_y = 18$ after eliminating the dispersion phase. $z_a = -1.819$ μm and $z_p = -1.663$ μm.

position of z_a always existed on the left-hand of an exact position of z_p. In order to make a continuous surface profile, for the measurement points in the region B a value of −0.320 μm was added to the measured value of z_p. Similarly, in the region C a value of −0.320 μm was subtracted from the measured value of z_p to obtain an exact position. This correction is called 2π phase correction as reported in Ref. [2]. A surface profile after the 2π phase correction is shown in Fig. 12, where the tilt and piston components were eliminated again. It was estimated that a curvature in the x direction in Fig. 12 was caused by a small deformation occurring after fixing the reference mirror with glue. But the measured surface profile was very smooth, and the magnitude of the small variations was less than 4 nm. In order to confirm clearly the small variations, Fig. 13 shows one-dimensional distribution along N_x at $N_y = 20$ in the surface profile of Fig. 12. The repeatability was obtained by calculating a root-mean-square value of the difference between two surface profiles measured in an interval of about 10 min. The repeatability was 1.2 nm in the measurement by z_p, while it was 13.2 nm in the measurement by z_s. It was made clear that the measurement value z_p provides a more exact position of a reflecting surface than the measurement value z_s.

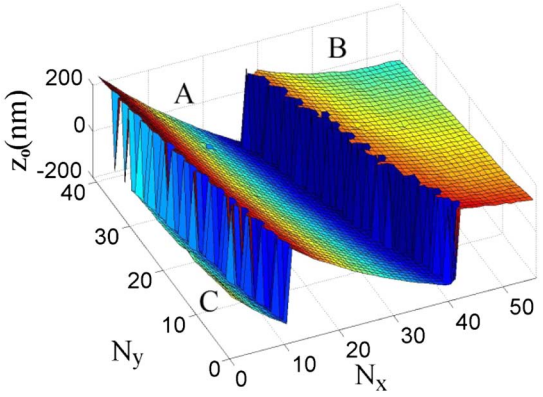

Fig. 10. Surface profile obtained from the measured values of z_p by using Eq. (7).

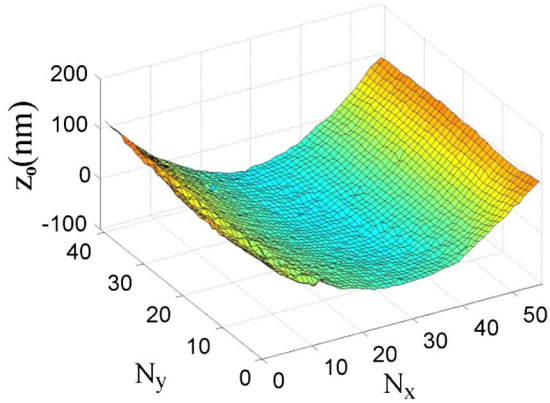

Fig. 12. Surface profile obtained from Fig. 9 after the 2π phase correction.

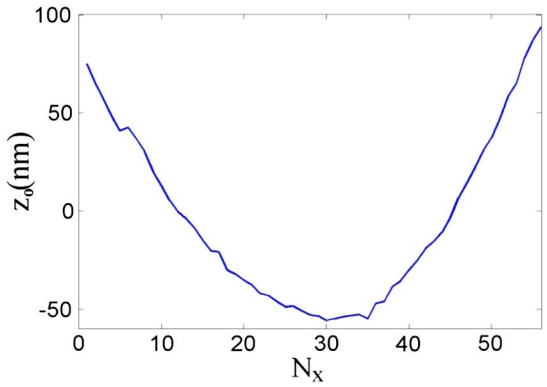

Fig. 13. One-dimensional distribution along N_x at $N_y = 20$ in the surface profile of Fig. 12.

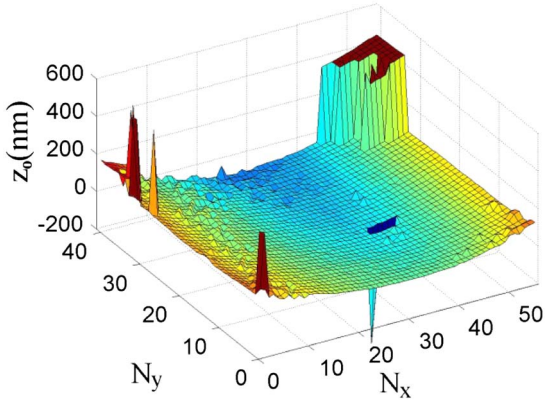

Fig. 14. Surface profile obtained from the measured values of z_p without eliminating the dispersion phase after the 2π phase correction.

In order to be sure of the requirement of eliminating the dispersion phase, a surface profile was obtained without eliminating the dispersion phase. This surface profile after the 2π phase correction is shown in Fig. 14. Although the 2π phase correction was performed, there were still spike-like variations with height more than 0.320 μm. And also there was a step-like variation with width more than 0.320 μm in the upper-right corner of region B. It was confirmed that the elimination of the dispersion phase is required to get an exact surface profile.

In order to examine the effectivity of using Eq. (7), a surface profile S_{one} was obtained by using one dispersion phase at $N_x = 30$ for all of the measurement points. The difference between this surface profile S_{one} and the surface profile of Fig. 12 is shown in Fig. 15. The difference values on the line of $N_x = 30$ are equal to zero, and the absolute value of the difference increases as the measurement position goes away from the line of $N_x = 30$. Moreover many spike-like variations appeared near the boundaries between the two regions shown in Fig. 10. These variations were caused by the fact that the step change occurred at different measurement positions between the surface profile of S_{one} and the surface profile of Fig. 12. Hence it is estimated that the dispersion phase or the aberration phase has some relations with the measurement position where

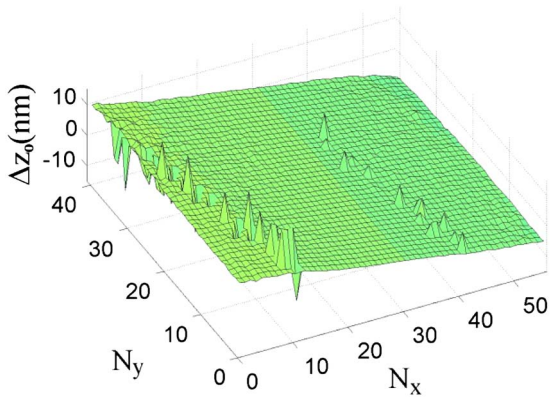

Fig. 15. Difference between the surface profile of Fig. 11 and the surface profile obtained by using a dispersion phase at $N_x = 30$ in Eq. (7) for all of the measurement points.

the step change occurs. Considering that the measurement error in the surface profile of Fig. 12 was less than 4 nm, the existence of the absolute values more than 4 nm in the difference of Fig. 15 indicates that the measurement error increases in the surface profile S_{one}. These results make it clear that the dispersion phase given by Eq. (7) is required to get an accurate surface profile with measurement error less than 4 nm.

4. CONCLUSION

The CVISs of the WLSI and the SRI were obtained from the real-valued interference signals through Fourier transform. First, the phase distribution in the CVIS of the SRI indicated the dispersion phase caused by the two sides of unequal length in the BS, and it was shown by the experiments that the magnitude of the dispersion phase changed linearly along the horizontal direction of the BS. Next the surface profile measurements were made with the WLSI. The dispersion phase with a different magnitude was subtracted from the spectral phase in Fourier transform of the real interference signal of the WLSI. Through inverse Fourier transform of this spectral distribution the dispersion-free CVIS was obtained, and the position z_p of zero phase nearest to the position z_a of amplitude maximum provided an accurate surface profile with an error less than 4 nm after the 2π correction, while the surface profile obtained by the position z_s calculated by the linear component of the spectral phase contained errors less than 12 nm. It was made clear that the utilization of the CVIS of the WLSI and SRI allows achieving highly accurate measurements of surface profile.

In order to get more accurate surface profiles it is required to investigate in more details how the positions of z_a and z_p are determined from the spectral distribution and also what kind of method is better to compensate the step change occurring in the measured value of z_p in the CVIS. These investigations will be carried out in the near future.

Funding. National Natural Science Foundation of China (NSFC) (11674111, 61575070); Promotion Program for Young and Middle-aged Teachers in Science and Technology Research of Huaqiao University (ZQN-PY209).

REFERENCES

1. M. C. Park and S. W. Kim, "Direct quadratic polynomial fitting for fringe peak detection of white light scanning interferograms," Opt. Eng. **39**, 952–959 (2000).
2. A. Harasaki, J. Schmit, and J. C. Wyant, "Improved vertical-scanning interfermetry," Appl. Opt. **39**, 2107–2115 (2000).
3. T. Pikálek, T. Fořt, and Z. Buchta, "Detection techniques in low-coherence interferometry and their impact on overall measurement accuracy," Appl. Opt. **53**, 8463–8470 (2014).
4. P. Lehmann, "Systematic effects in coherence peak and phase evaluation of signals obtained with a vertical scanning white-light Mirau interferometer," Proc. SPIE **6188**, 618811 (2006).
5. P. de Groot and L. Deck, "Surface profiling by analysis of white-light interferograms in the spatial frequency domain," J. Mod. Opt. **42**, 389–401 (1995).
6. P. de Groot, X. C. de Lega, J. Kramer, and M. Turzhitsky, "Determination of fringe order in white-light interference microscopy," Appl. Opt. **41**, 4571–4578 (2002).
7. M. B. Sinclair, M. P. de Boer, and A. D. Corwin, "Long-working-distance in-coherent-light interference microscope," Appl. Opt. **44**, 7714–7721 (2005).
8. S. Luo, O. Sasaki, Y. Liu, X. Li, Z. Lin, and J. Pu, "Elimination of dispersion effect in white-light scanning interferometer by a spectral analyzer," Opt. Rev. **24**, 27–32 (2017).
9. S. S. C. Chim and G. S. Kino, "Three-dimensional image realization in interference microscopy," Appl. Opt. **31**, 2550–2553 (1992).